Spectrochimica Acta Part A 83 (2011) 279–287

Contents lists available at SciVerse ScienceDirect

Spectrochimica Acta Part A: Molecular and Biomolecular Spectroscopy

journal homepage: www.elsevier.com/locate/saa

Significant modification of the I^-_3 Lewis base character in the β-cyclodextrin polyiodide inclusion complex with Co^{2+} ion: An FT-Raman investigation

Vasileios G. Charalampopoulos[a,*], John C. Papaioannou[a,**], Athanasios A. Tsekouras[a], Glikeria Kakali[b], Haido S. Karayianni[c]

[a] Laboratory of Physical Chemistry, Department of Chemistry, National and Kapodistrian University of Athens, 157 71 Zografou, Athens, Greece
[b] Laboratory of Inorganic and Analytical Chemistry, School of Chemical Engineering, National Technical University of Athens, 15780 Zografou, Athens, Greece
[c] Laboratory of Physical Chemistry, School of Chemical Engineering, National Technical University of Athens, 15780 Zografou, Athens, Greece

ARTICLE INFO

Article history:
Received 31 March 2011
Received in revised form 15 August 2011
Accepted 19 August 2011

Keywords:
β-Cyclodextrin inclusion complex
Raman spectroscopy
Heptaiodides
Charge–transfer
Order–disorder

ABSTRACT

The β-cyclodextrin (β-CD) polyiodide inclusion complex $(\beta\text{-CD})_2\cdot Co_{0.5}\cdot I_7\cdot 21H_2O$ has been synthesized, characterized and further investigated via FT-Raman spectroscopy in the temperature range of 30–120 °C. The experimental results point to the coexistence of I^-_7 units ($I_2\cdot I^-_3\cdot I_2$) that seem not to interact with the Co^{2+} ions and I^-_7 units that display such interactions. The former units exhibit a disorder–order transition of both their I_2 molecules above 60 °C due to a symmetric charge–transfer interaction with the central I^-_3 [$I_2 \leftarrow I^-_3 \rightarrow I_2$], whereas in the latter units only one of the two I_2 molecules becomes well-ordered above 30 °C. The other I_2 molecule remains disordered presenting no charge–transfer phenomena. The Co^{2+} ion induces a considerable asymmetry on the geometry of the I^-_3 anion and a significant modification of its Lewis base character. Complementary dielectric measurements suggest no important involvement of H···I contacts in the observed modification of the I^-_3 electron-transfer properties.

1. Introduction

It is well known that α-, β- and γ-cyclodextrins (α-, β-, γ-CDs) exhibit the fascinating ability to act as hosts to numerous inorganic and organic guest components forming stable inclusion complexes of well-defined stoichiometry [1]. Despite the fact that a vast variety of such systems have comprised the subject of in-depth experimental and theoretical investigations over the years, little work has been reported [2–6] on the physicochemical properties of the crystallographically characterized [7–10] α-CD and β-CD polyiodide inclusion complexes with different metal ions (named (α-CD)-M and (β-CD)-M, respectively, M stands for the corresponding metal). Our recent studies [11–18] have been exclusively focused on these crystalline materials since: (i) the highly disordered H-bonding networks are of great biological importance [19,20], (ii) polyiodides display potential technical applications in a wide range of areas such as electronics, optical devices, batteries etc. [21,22], and (iii) host–guest interactions play a fundamental role in the intriguing fields of molecular recognition, self-assembly and supramolecular chemistry in general [6,23].

Aiming at a profound understanding of the underlying phenomena that appear in the aforementioned complexes as a function of temperature, we have combined several experimental techniques. Interestingly enough, dielectric spectroscopy and thermal analysis have shed light not only on the dipolar (H_2O, –OH) and metal ion fluctuations in the interstitial spaces between the neighboring CD stacks (head to head arranged CD dimers) but also on the extensive electron delocalization along the disordered polyiodide chains which are embedded in the CD tubular cavities. These endless chains are composed of weakly interactive I^-_5 ions in (α-CD)-M [7–9,14,15,18] and non-interactive I^-_7 ions in (β-CD)-M [10–13,16,17]. The examination of the nature of the polyiodide subunits has been carried out by means of FT-Raman spectroscopy. This method has offered valuable information on the evolution of the intra/intermolecular interactions of the individual building blocks during the thermal variation of the samples under research by allowing us to observe a series of detailed snapshots of all the relevant structural conversions.

Concerning (β-CD)-M complexes where the I atoms of the two I_2 molecules of each heptaiodide ($I_2\cdot I^-_3\cdot I_2$) are disordered in positions of main and minor occupancies [10], the obtained FT-Raman data have revealed the following [11–13,16,17]: (i) through slow heating both the I_2 molecules of I^-_7 gradually become elongated and well-ordered (disorder–order transition) due to a thermally activated charge–transfer interaction with the central I^-_3 ion [$I_2 \ldots I^-_3 \ldots I_2$], and (ii) the symmetry as well as the extent of the electron

* Corresponding author.
** Corresponding author. Tel.: +30 210 7274561.
E-mail addresses: v_charalampopoulos@yahoo.gr (V.G. Charalampopoulos), jpapaioannou@chem.uoa.gr (J.C. Papaioannou).

1386-1425/$ – see front matter © 2011 Elsevier B.V. All rights reserved.
doi:10.1016/j.saa.2011.08.031

donating properties of I^-_3 (Lewis base character) appear to depend on each metal ion's relative position and ionic potential q/r (q is the charge and r the ionic radius [24]), respectively. As regards metal ions with an ionic potential that is lower than ~1.50, they seem not to affect the Lewis base character of I^-_3 which displays a symmetric and full charge–transfer interaction with the two I_2 molecules [$I_2 \leftarrow I^-_3 \rightarrow I_2$]. Nevertheless, when the ionic potential of the metal ions is greater than ~1.50, the M^{n+}...I^-_3 interactions have proven to become significant. In the case of a face-on position of M^{n+} in relation to I^-_3, the charge–transfer interaction of the latter one with both the I_2 molecules is attenuated but remains symmetric [$I_2 \leftarrow I^-_3 \rightarrow I_2$], whereas in the case of a side-on position of M^{n+} in relation to I^-_3, the above charge–transfer interaction becomes non-symmetric [$I_2 \leftarrow I^-_3 \rightarrow I_2$].

In the present work, we carry out the synthesis, characterization and high temperature (30–120 °C) FT-Raman spectroscopic study of the β-CD polyiodide inclusion complex with cobalt ion ((β-CD)-Co). Our main aim is the elucidation of the temperature-dependent I^-_7 structural changes in order to obtain valuable insights into the Co^{2+}...I^-_3 interactions and the emerging modification of the I^-_3 Lewis base character. Additionally, complementary dielectric measurements are conducted for the determination of the extent of the disorder phenomena in the corresponding hydrogen-bonding network.

2. Experimental

2.1. Materials and synthesis

β-CD and solid iodine were obtained from Fluka Chemica whereas cobalt iodide (CoI_2) was obtained from Alfa Aesar. β-CD, 1.0 g, (0.881 mmol) was dissolved in distilled water (80 mL) at room temperature with continuous stirring (full dissolution). Then, 0.36 g of cobalt iodide (1.151 mmol) and 0.44 g of solid iodine (1.733 mmol) were simultaneously added to the solution which was heated to 70 °C for 20–25 min. The hot solution was quickly filtered through a folded filter paper into an empty beaker (100 mL) which was covered with Teflon and then immersed in a Dewar flask (500 mL) containing hot water at the same temperature. After 2 days, reddish–brown crystals of (β-CD)-Co had grown which were isolated by filtration and dried in air.

2.2. Simultaneous thermal analysis (STA), elemental analysis and X-ray powder diffraction (XRPD)

Simultaneous thermogravimetry analysis (TGA) and differential thermal analysis (DTA) of the crystals were conducted using a NETZSCH-STA 409 EP Controller TASC 414/3 (reference Al_2O_3). Both the weight variation of the sample (68.70 mg) and the relevant endothermic transitions were recorded during heating from 23 to 148 °C with a heating rate of 5 °C min^{-1} under a dynamic nitrogen atmosphere.

The C and H contents of the inclusion complex were determined microanalytically on a Perkin–Elmer 2400 Series II CHNS/O Elemental Analyzer (combustion analysis) operating in the CHN mode. The Oxygen mode could not be used due to the presence of metal ions in the sample. The Co content was measured on a Perkin–Elmer Elan 6100 ICP-MS (inductively coupled plasma-mass spectrometer).

The X-ray powder diffraction pattern was obtained with a Siemens D 5000 diffractometer using monochromatized Cu Kα1 radiation of λ = 1.54059 Å (monochromator: graphite crystal) at 40 kV and 30 mA. The diffraction data were collected in the 2θ range of 5–55° with a constant step of 0.015° and a dwell time of 5 s/step. The calculation of the simulated X-ray powder diffraction pattern of $(\beta\text{-CD})_2{\cdot}KI_7{\cdot}9H_2O$ [10] was performed by means of the computer program POWDERCELL 2.4 developed by Nolze and Kraus [25,26].

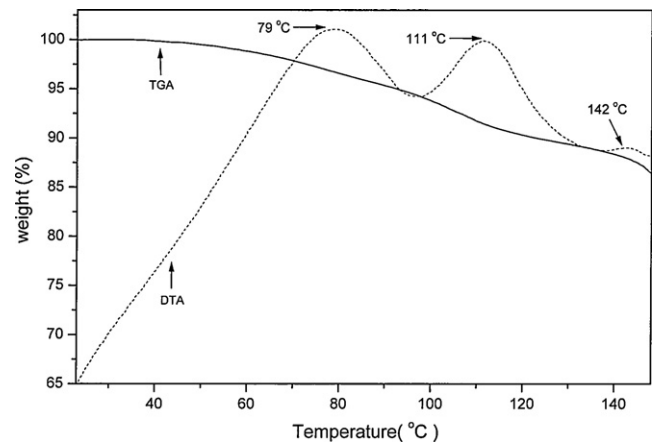

Fig. 1. Simultaneous thermogravimetry (TGA) and differential thermal analysis (DTA) of $(\beta\text{-CD})_2{\cdot}Co_{0.5}{\cdot}I_7{\cdot}21H_2O$ with a heating rate of 5 °C min^{-1}.

2.3. FT-Raman spectroscopy

The Raman spectra were obtained at 4 cm^{-1} resolution from 3500 cm^{-1} to 100 cm^{-1} with a data point interval of 1 cm^{-1} using a Perkin–Elmer NIR FT-spectrometer (Spectrum GX II) equipped with an InGaAs detector. The laser power and spot (Nd: YAG at 1064 nm) were controlled to be constant at 50 mW during the measurements and 400 scans were accumulated. The solid sample was packed into a suitable stationary cell and the low laser power was used in order to prevent both photochemical and thermal decomposition by the laser beam. During gradual heating from 30 to 120 °C the temperature was raised in 10 °C increments in the range of 30–70 °C, in 5 °C increments in the range of 70–100 °C, and in 10 °C increments in the range of 100–120 °C. The temperature variation was controlled with a Ventacon Winchester instrument equipped with a CALCOMMS 3300 autotune controller.

2.4. Dielectric spectroscopy

For the dielectric measurement, a pressed pellet of powdered sample (544.6 mg) 20 mm in diameter with thickness 1.06 mm was prepared with a pressure pump (Riken Powder model P-1B) at room temperature. Two platinum foil electrodes were pressed at the same time with the sample. The pellet was then loaded into a temperature-controlled chamber, between two brass rods accompanied by a compression spring. The electrical data were obtained using a low-frequency (0–100 kHz) dynamical signal analyzer (DSA-Hewlett-Packard 3561A) at the temperature range of 108.0–308.0 K (slow heating).

3. Results and discussion

3.1. Characterization of the synthesized inclusion complex

The TGA and DTA curves of (β-CD)-Co from room temperature to 148 °C (heating rate: 5 °C min^{-1}) are shown in Fig. 1. The number of crystalline water molecules per β-CD dimer was calculated from the weight loss (10.69%) in the temperature range of ~42–131 °C, where the dehydration process progressively takes place. The result is consistent with ~21 water molecules per dimer by taking into account the general composition $(\beta\text{-CD})_2{\cdot}MI_7{\cdot}nH_2O$ (M stands for the metal ion) that has been described for all the inclusion complexes of the family [10–13,16,17]. The two strong

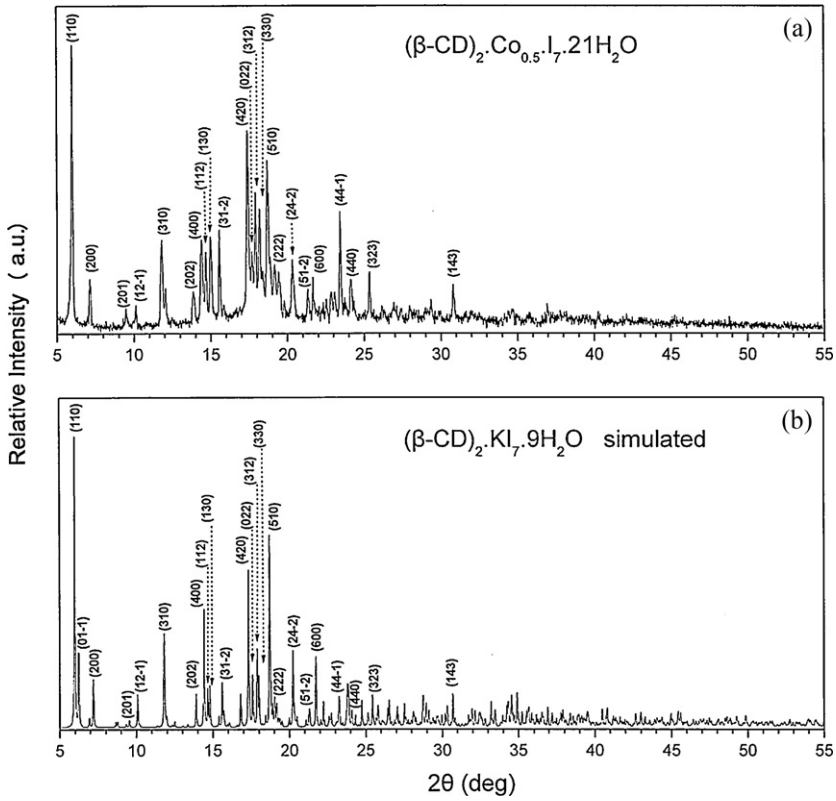

Fig. 2. (a) Experimental X-ray powder diffraction pattern of $(\beta\text{-CD})_2{\cdot}Co_{0.5}{\cdot}I_7{\cdot}21H_2O$ at room temperature and (b) simulated X-ray powder diffraction pattern of $(\beta\text{-CD})_2{\cdot}KI_7{\cdot}9H_2O$ calculated from the respective single crystal data [10].

endothermic peaks at 79 and 111 °C, conform with the gradual removal of the two coexistent kinds of H_2O molecules and this discrimination is explained by the following discussion. In the interstices of the crystal lattice, some of the water molecules are positionally disordered displaying extensive thermal motions (easily movable state) whereas others are neatly coordinated with fully occupied positions (tightly bound state) reflecting differences in the corresponding local environments. Through slow heating, the energy content of the interstitial water arrangement continuously increases resulting in the loss of the disordered water molecules at lower temperatures (79 °C) than those at which the loss of the well-ordered ones occurs (111 °C). The third endothermic peak at 142 °C is assigned to the sublimation of I_2 which involves the degradation of polyiodide moieties and the extensive electron delocalization along the chain length [11–18]. Furthermore, we have carried out the compositional analyses of Co, C and H elements for the following reasons: (i) to determine the quantitative relationship between the cobalt ions and the β-CD dimers of the inclusion complex; this is a prerequisite for the thorough interpretation of the metal ions' effect on the polyiodide charge–transfer phenomena (studied via FT-Raman spectroscopy), and (ii) to verify the validity of the water content estimated from the TGA/DTA data (Fig. 1) in order to eliminate the possibility of any partial loss of iodine in the range of ~42–131 °C. The experimental results are: Co, 0.76%; C, 28.20%; H, 5.21% (Co to C to H ratio: 1:37.10:6.85). In view of the general composition $(\beta\text{-CD})_2{\cdot}MI_7{\cdot}nH_2O$ the respective theoretical values are: Co, 1.64%; C, 28.06%; H, 5.10% (Co to C to H ratio: 1:17.11:3.11). It is clearly evident that both the experimental %Co value and the relevant Co to C to H ratio significantly differ from the corresponding theoretical ones suggesting that the crystal lattice does not exhibit 1.0 cobalt ion per β-CD dimer. Considering a statistical distribution of 0.5 Co^{2+} per β-CD dimer ($(\beta\text{-CD})_2{\cdot}M_{0.5}{\cdot}I_7{\cdot}nH_2O$) the already calculated degree of hydration from the thermal analysis data (Fig. 1) remains unchanged ($n = \sim 21$ H_2O) whereas the resultant theoretical Co, C and H contents are: Co, 0.83%; C, 28.29%; H, 5.14% (Co to C to H ratio: 1:34.08:6.19). It becomes apparent that the experimental values obtained as well as the relevant Co to C to H ratio are in very good agreement with the theoretical ones for a statistically distributed cobalt ion (0.5 Co^{2+} per dimer). Therefore, the general composition of (β-CD)-Co can be described as $(\beta\text{-CD})_2{\cdot}Co_{0.5}{\cdot}I_7{\cdot}21H_2O$.

The X-ray powder diffraction (XRPD) pattern of (β-CD)-Co at ambient temperature along with the simulated pattern of $(\beta\text{-CD})_2{\cdot}KI_7{\cdot}9H_2O$ ((β-CD)-K) calculated from the respective single crystal data [10] are shown in Fig. 2a and b. It is obvious that all the well-distinguishable Bragg reflections ($h\,k\,l$) of the experimental XRPD pattern are located at positions (2θ angles) identical to those of the reflections in the theoretical pattern implying that (β-CD)-Co is isomorphous to (β-CD)-K displaying a monoclinic crystal form with space group $P2_1$ [10]. The relative reflection intensities in the XRPD pattern of (β-CD)-Co differ from the corresponding ones in the pattern of (β-CD)-K as a result of: (i) the much higher degree of hydration of (β-CD)-Co (21 H_2O per dimer) in comparison to that of (β-CD)-K (9 H_2O per dimer) indicating that the co-crystallized water molecules of these two systems are neither expected to occupy equivalent lattice positions nor to present identical spatial correlations, (ii) the structural differences between the I^-_7 ions of (β-CD)-Co and (β-CD)-K (as evident from the FT-Raman investigation) which emerge from the individual nature of each counterion along with slight variations during synthesis and crystallization, (iii) an inevitable though little contribution of texture effects, and (iv) the different scattering powers of cobalt and potassium ions accompanied by their different distributions in the relevant crystal lattices. Moreover, we report that the total absence of any hump (indicative of amorphous material) in the experimental XRPD

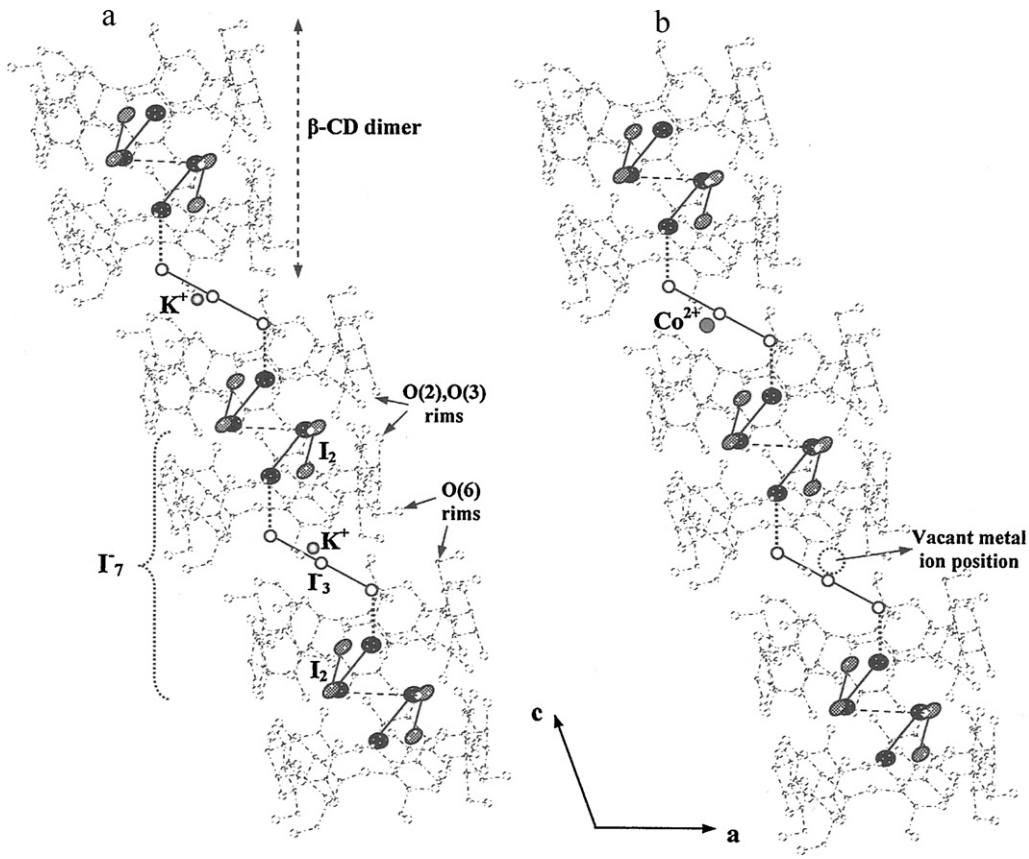

Fig. 3. (a) The crystalline structure of the polyiodide inclusion complex $(\beta\text{-CD})_2\cdot KI_7\cdot 9H_2O$, viewed along the *b*-axis and based on the single-crystal X-ray analysis carried out by Betzel et al. [10]. In every space between the O(6) rims of the neighboring β-CD dimers a K^+ ion is located. The Z-shaped I^-_7 ions ($I_2\cdot I^-_3\cdot I_2$) are embedded in the β-CD dimers. The well-ordered I atoms of I^-_3 are presented as white spheres. The I_2 units consist of disordered I atoms in positions of minor (d(I–I) < 2.77 Å) and main occupancies (d(I–I) = ~2.77 Å) [10] that are presented as spotty gray and black ellipsoids, respectively. The K^+ ions are presented as gray spheres. (b) Schematic representation of the statistical distribution of Co^{2+} ions (0.5 Co^{2+} per dimer) in the polyiodide inclusion complex $(\beta\text{-CD})_2\cdot Co_{0.5}\cdot I_7\cdot 21H_2O$. For each space between the O(6) rims of two neighboring β-CD dimers where a Co^{2+} ion is located, another respective space is expected to lack the presence of a Co^{2+} ion (vacant metal ion position).

pattern proves the purity of the synthesized inclusion complex (single phase).

The observed isomorphism reveals that the cobalt ions exhibit similar coordination schemes to those described for potassium ions in the single crystal X-ray diffraction study of (β-CD)-K by Betzel et al. [10]. However, the elemental analysis data (0.5 Co^{2+} per dimer) suggest that the former ions do not display exactly the same structural motif as that of the latter ones. As regards the crystal structure of (β-CD)-K [10], in every space between the O(6) rims of the neighboring β-CD dimers along each β-CD stack, one K^+ ion was found to be located (coordinated with H_2O molecules and O(6)H groups outside the CD annuli) opposite to the central I^-_3 ion of the enclosed Z-shaped I^-_7 units (Fig. 3a). In the present case, the statistical distribution of the cobalt ions can be interpreted as follows: for each space between the O(6) rims of two neighboring dimers where a Co^{2+} ion is located there is another respective space between two other β-CD dimers which lacks the presence of a Co^{2+} ion (Fig. 3b). The fractional coordinates of the Co^{2+} ions as well as the specific spatial correlation between their lattice positions and the vacant Co^{2+} ion positions in the unit cell of (β-CD)-Co can only be determined by means of detailed crystallographic analysis which is beyond the scope of the current work. Nevertheless, a coexistence of I^-_7 units which interact with the Co^{2+} ions and I^-_7 units which present no such interactions should be expected. This consideration is further confirmed by the high temperature FT-Raman spectra of (β-CD)-Co.

3.2. FT-Raman spectroscopy

The FT-Raman spectra of (β-CD)-Co in the temperature range of 30–120 °C are shown in Fig. 4a–c. For the interpretation of the spectral data obtained, the following points have been taken into account: (i) the increase of the characteristic intramolecular distance of solid I_2 (d(I–I) = 2.715 Å) as it becomes coordinated to a Lewis base donor (electron density donation to its σ^* antibonding orbital) along with the consequent shift of its Raman-active ν_1 mode at 180 cm^{-1} to lower frequencies (decreased I_2 force constant) [22,27], (ii) the empirical correlation between the vibrational frequency ν(I–I) and the intramolecular distance d(I–I) of I_2 in weak-medium strength charge–transfer (CT) compounds, suggested by Deplano et al. [28,29], and (iii) the concentration of the major part of the electron density of I^-_3 ion on its terminal iodine atoms [22,30,31]. At 30 °C, the strong band at 178 cm^{-1} and the easily distinguishable shoulder at 171 cm^{-1} reveal that in (β-CD)-Co there are disordered I_2 molecules which display different mean intramolecular distances $\bar{d}$(I–I) of ~2.72 (these molecules are denoted as (I)) and ~2.75 Å (denoted as (II)), respectively, reflecting differences in the occupancies of the corresponding I atoms. In the range of 30–50 °C, the band at 171 cm^{-1} becomes more intense while the one at 178 cm^{-1} becomes less intense indicating that the I_2 molecules (I) are gradually transformed into (II) ones (change of $\bar{d}$(I–I) from ~2.72 to ~2.75 Å) as the temperature is raised. The isosbestic point at 175 cm^{-1} provides further evidence of two discrete structures of disordered I_2 molecules which exchange population

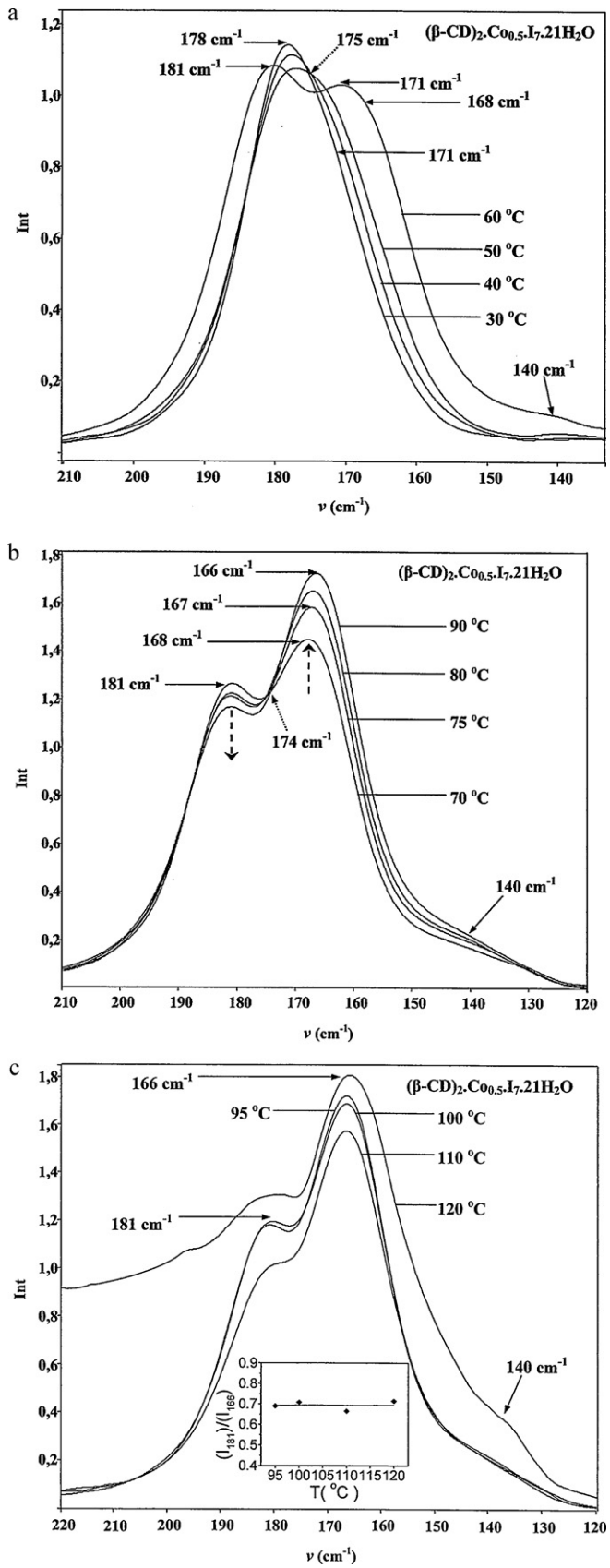

Fig. 4. Raman spectra of $(\beta\text{-CD})_2\cdot Co_{0.5}\cdot I_7\cdot 21H_2O$ during heating, in the temperature ranges of (a) 30–60 °C, (b) 70–90 °C, and (c) 95–120 °C. The inset in (c) highlights the almost constant Raman intensity ratio $(I_{181})/(I_{166})$ in the range of 95–120 °C.

via the slow heating of the crystals [32]. The downshift of the band at 178 cm^{-1} is considered to result from the initiation of the elongation of the disordered I_2 molecules (I) (disorder–order transition) due to a thermally activated charge–transfer interaction with the I^-_3 Lewis base donor. This behavior seems rather peculiar since in our previous studies the polyiodide charge–transfer phenomena in (β-CD)-M complexes have proven to begin at higher temperatures (T = ~70 °C) [11–13,16,17].

At 60 °C, what becomes obvious is the presence of two strong bands at 181 and 171 cm^{-1} and a shoulder at 168 cm^{-1}. The band at 181 cm^{-1} exists from the beginning of the experiment but is masked by the initial band at 178 cm^{-1} and its appearance reveals that there are also disordered I_2 molecules with d(I–I) = ~2.71 Å (denoted as (III)). The shoulder at 168 cm^{-1}, apart from showing that the elongation of the I_2 molecules (I) is still in progress it may further comprise evidence for the initiation of the elongation of I_2 molecules (II) due to a charge–transfer interaction with I^-_3. From 60 to 90 °C, the shoulder at 168 cm^{-1} and the band at 171 cm^{-1} are gradually shifted to the final frequency of 166 cm^{-1} implying that the disordered I_2 molecules (I) and (II) progressively become well-ordered exhibiting a final intramolecular distance of ~2.77 Å. The intermediate states of the I_2 bond lengthening are responsible for the intermediate bands observed at 168 and 167 cm^{-1}. Moreover, in the aforementioned temperature region, the continuously decreased intensity of the band at 181 cm^{-1} in combination with the continuously increased intensity of the intermediate bands and the final band at 166 cm^{-1} suggest that the disordered I_2 units (III) undergo a disorder–order transition as well presenting a final intramolecular distance of ~2.77 Å. The isosbestic point at 174 cm^{-1} supports the evolution of such an underlying process. From 95 to 120 °C, the intensity ratio of the bands at 181 and 166 cm^{-1} remains almost invariant (inset in Fig. 4c) and the fact that the former band is retained without being downshifted in this range implies the existence of disordered I_2 molecules that do not display either charge–transfer effects with I^-_3 or a disorder–order transition (denoted as (IV), d(I–I) = ~2.71 Å).

The spectral features described above are consistent with the coexistence of two discrete types of heptaiodide units in (β-CD)-Co. The gradual shifts of the bands at 171 and 181 cm^{-1} to the final frequency of 166 cm^{-1} are attributed to the disorder–order transition of the I_2 molecules of the I^-_7 units which seem not to interact with the Co^{2+} ions (Fig. 5). In some of these I^-_7 units, the I_2 molecules display a mean intramolecular distance d(I–I) of ~2.71 Å ((III)) whereas in others a d(I–I) of ~2.75 Å ((II)). This makes sense, if we take into consideration that real crystals deviate from the ideal picture of a periodical perfect repetition of a unit cell [33]. Both (II) and (III) are disordered exhibiting I atoms which are distributed in positions of main and minor occupancies. The single crystal X-ray analysis of the isomorphous (β-CD)-K [10] has shown that for the positions of main occupancies d(I–I) = ~2.77 Å (for the positions of the minor occupancies the relevant d(I–I) was not estimated). This finding has been validated not only for (β-CD)-K but also for a series of (β-CD)-M inclusion complexes by our recent vibrational spectroscopy investigations [11–13,16,17]. At ~70 °C, a symmetric and full charge–transfer interaction begins between the central I^-_3 ion and the two I_2 molecules [$I_2 \leftarrow I^-_3 \rightarrow I_2$] of the aforementioned I^-_7 units resulting in the complete ordering of the disordered I atoms of (II) and (III) at the corresponding positions of main occupancies (well-ordered state, d(I–I) = ~2.77 Å). Such an interpretation conforms with a centrosymmetric ($D_{\infty h}$ symmetry, r1 = r2) or nearly centrosymmetric I^-_3 ion indicating an equal distribution of the electron density between its two terminal iodine atoms I(1), I(3) (Fig. 5) and an ability of the latter ones to act as Lewis base donors to the same extent [22,30,31]. Furthermore, experimental and theoretical studies on a series of solid polyiodide systems have shown that the characteristic Raman-active ν_1 mode of a centrosymmetric

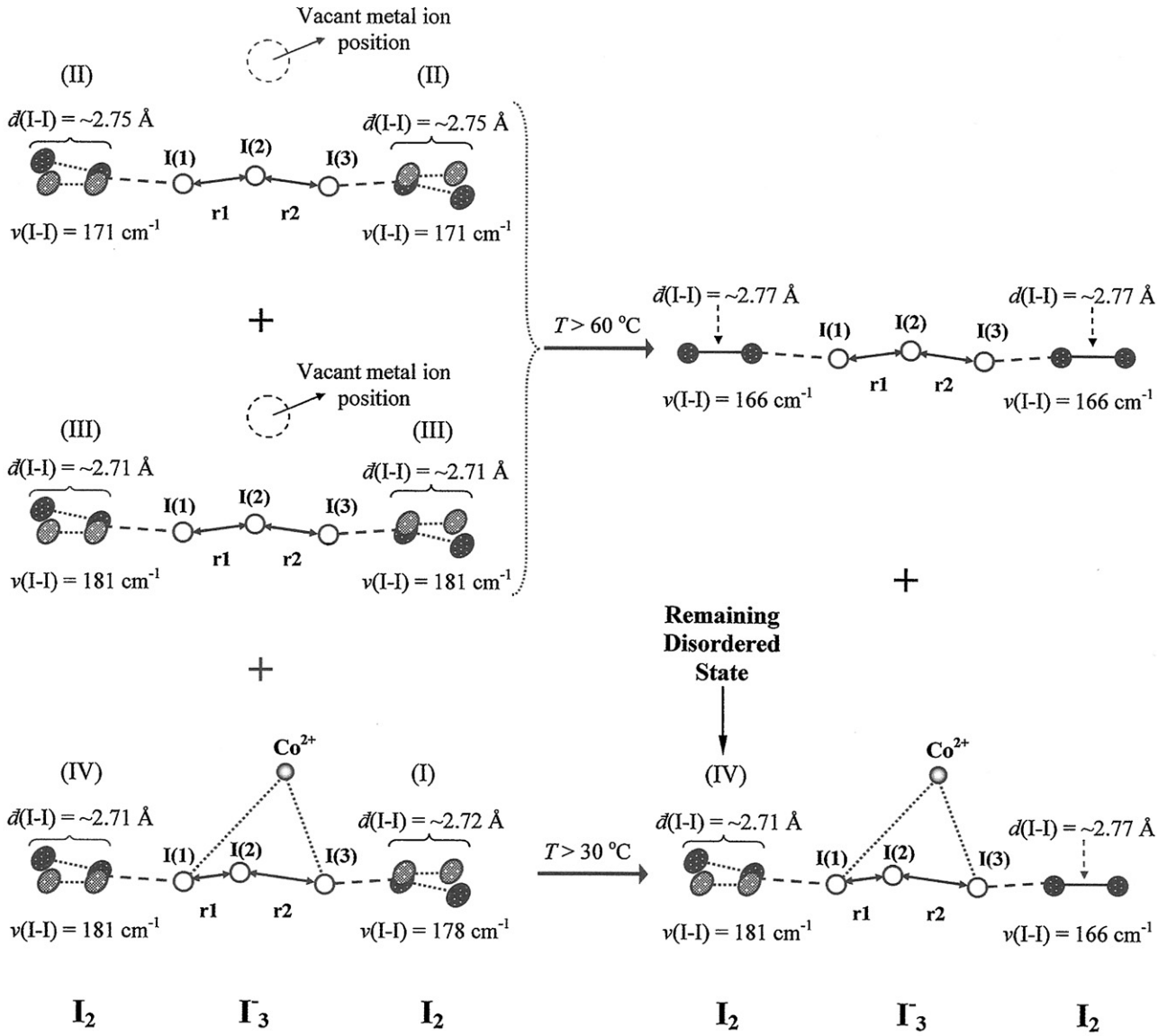

Fig. 5. The thermal variations of the I_2 molecules in $(\beta\text{-CD})_2\cdot Co_{0.5}\cdot I_7\cdot 21H_2O$. The I^-_7 units ($I_2\cdot I^-_3\cdot I_2$) are viewed along the *a*-axis whereas the β-CD molecules are omitted for the sake of clarity. Above 60 °C, the I_2 molecules (II) and (III) of the I^-_7 units which present no interactions with the Co^{2+} ions (vacant metal ion position) display a disorder–order transition due to a symmetric charge–transfer interaction with the central I^-_3 (r1 = r2). In the case of the I^-_7 units which interact with the Co^{2+} ions, the latter ones seem to occupy a side-on position in relation to I^-_3 (r2 > r1). Above 30 °C, the I_2 molecules (I) undergo a disorder–order transition due to a charge–transfer interaction with the I(3) terminal atom of I^-_3. On the contrary, the I_2 molecules (IV) remain in the disordered state exhibiting no charge–transfer interaction with the I(1) terminal atom of I^-_3.

I^-_3 with r1 = r2 ≈ 2.90–2.92 Å or a nearly centrosymmetric I^-_3 with (r1 + r2) ≈ 5.80–5.85 Å appears at the narrow frequency range of ~105–110 cm^{-1} [4,22,34–37]. The present (r1 + r2) length is longer than 6.00 Å [10] and this band is expected to be located near or below 100 cm^{-1} [38] in the spectra of (β-CD)-Co. Thus, it could not be detected due to the limited frequency range of the spectrometer (≥100 cm^{-1}).

In the case of the I^-_7 units which interact with the Co^{2+} ions the situation is more complicated. The two coexistent bands at $T > 95$ °C, suggest a side-on position of Co^{2+} in relation to I^-_3 (Fig. 5) and a remarkable influence of the cation on the electron donating properties of the anion. Taking into consideration that the ionic potential q/r of Co^{2+} is 2.70 ($q = +2$, $r = 0.74$ Å), the above explanation is in accordance with our recent work which demonstrated that the $M^{n+}\ldots I^-_3$ interactions in (β-CD)-M systems become strong when the ionic potential of the cation is greater than ~1.50 [16]. The terminal I atom of I^-_3 nearest to the cobalt ion (I(3)), is expected to exhibit a greater negative charge (electron density) than the other terminal I atom (I(1)) whereas the intramolecular I–I distance (r2) nearest to the cobalt ion is expected to be longer than the other intramolecular I–I distance (r1) [30,39]. However, since the disordered I_2 molecules (IV) do not undergo any disorder–order transition, it becomes apparent that the I(1) terminal atom does not possess any considerable electron density and consequently it cannot act as a Lewis base donor. On the other hand, the unexpected initiation of the disorder–order transition of the I_2 molecules (I) (178 → 166 cm^{-1}) in the low temperature range of 30–40 °C makes clear that the major part of the electron density of I^-_3 is concentrated on the I(3) terminal atom which exhibits a tremendously increased tendency to act as a Lewis base donor. Thus, the I^-_3 ion appears to be highly asymmetric presenting a large distortion (Δd = r2–r1 > 0.1 Å) [22]. This conclusion is further confirmed by the existence of the weak band at 140 cm^{-1} (Fig. 4a–c), which is assigned to the ν_3 asymmetric stretch (125–150 cm^{-1}) of the I^-_3

ion [22,34,39–42]. As it is already known, the ν_3 vibrational mode (along with the bending mode ν_2 at ~50–70 cm^{-1}) of a centrosymmetric I^-_3 ion ($D_{\infty h}$) is IR-active and Raman forbidden [22]. The fact that, in the present case, this mode has become Raman-active indicates the important lowering of the I^-_3 symmetry. For this reason, the electron donating ability of I^-_3 is amplified in the r2 direction (electron transfer to (I)) and totally diminishes in the r1 direction (no electron transfer to (IV)). Such a significant modification of the Lewis base character of I^-_3 was not observed in the previously investigated (β-CD)-M complexes whose metal ions (Li^+, Cd^{2+}, V^{3+}) appeared to occupy side-on relative positions [16]. Even in the case of the V^{3+} ion, which displays a greater ionic potential (q/r = 4.05) than that of Co^{2+}, the I^-_3 ion was found to be weakly distorted (Δd = r2–r1 ≤ 0.1 Å). This finding was justified by: (i) the total absence of the corresponding ν_3 asymmetric stretch in the Raman spectra of (β-CD)-V, (ii) the verified ability of both the terminal I atoms of I^-_3 to act as Lewis base donors and (iii) the initiation of the I^-_7 charge–transfer interaction at ~75 °C. Therefore, it becomes obvious that Co^{2+} induces a larger distortion of the I^-_3 geometry than V^{3+} and the interpretation of this discrepancy relies on the balance between the cation's ionic potential and its tendency to interact with polyiodide species. More specifically, several studies on a series of iodide-selective membrane electrodes that contained the cobalt ion have repeatedly reported an extremely enhanced selectivity for I^- anions being attributed to a unique Co^{2+}. . . iodide interaction [43–45]. In our work, this specific behavior of Co^{2+} ion seems to play a key role in the noticeable perturbation of the bonding and electronic structure of I^-_3 and the resultant modification of its electron donating properties (total asymmetry). The ν_1 vibrational mode of the asymmetric I^-_3 ions is located near or below 100 cm^{-1} (non-detectable), providing evidence for an important increment of their total length (r1 + r2) due to their strong interionic interactions with Co^{2+}.

Finally, it is believed by the authors that dynamical phenomena are mainly involved in the disorder of all the existing I_2 units in the crystal lattice of (β-CD)-Co; in such a case, the lifetime of the ground state is expected to be shorter than that of the Raman vibrational scale (10^{-13} s) [46] supporting the term "mean distance $\bar{d}$(I–I)" that has been adopted in the current research.

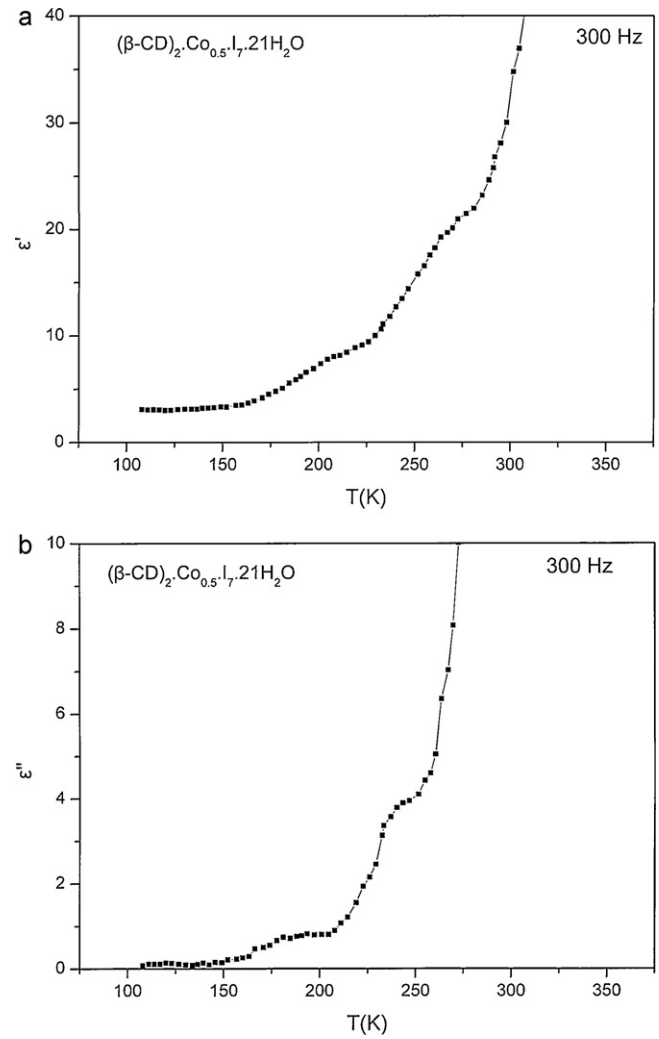

Fig. 6. Temperature dependence of (a) the real part ε' and (b) the imaginary part ε'' of the dielectric constant ε of $(\beta\text{-CD})_2{\cdot}Co_{0.5}{\cdot}I_7{\cdot}21H_2O$ at 300 Hz.

3.3. Dielectric spectroscopy

All the disorder phenomena that progressively appear in the hydrogen-bonding network of (β-CD)-Co over the temperature range of 108.0–308.0 K, are characterized in terms of the complex permittivity ε^* which is represented by the following relation [47]:

$$\varepsilon^*(f) = \varepsilon'(f) - j\varepsilon''(f) \quad (1)$$

where the real part ε' defines the capacitance of the sample, the imaginary part ε'' (loss factor) expresses the energy dissipation per cycle, f is the frequency of the applied electric field and $j = \sqrt{-1}$.

The temperature dependences of the real part ε' and the imaginary part ε'' at the low frequency of 300 Hz are shown in Fig. 6a and b. At T < 220.0 K, the sigmoid curve of low height ($\Delta\varepsilon'$ = 6.04, inflection point at 193.5 K) in the $\varepsilon'(T)$ variation as well as the flat bell-shaped curve (ε''_{max} = 0.81 at 193.5 K) in the $\varepsilon''(T)$ variation are attributed to the order–disorder transition (T_{trans} = 193.5 K) of some normal hydrogen bonds to those of flip-flop type according to the scheme:

$$\underset{\text{(normal H-bonds)}}{\text{O–H}\cdots\text{O–H}} \rightarrow \underset{\text{(flip-flop H-bonds)}}{\text{O–(1/2H)}\cdots\text{(1/2H)–O}} \quad (2)$$

Flip-flop hydrogen bonds have been originally detected in the single crystal of β-cyclodextrin hydrate (β-CD·11H_2O) at room temperature by means of neutron diffraction analysis [48,49] and exhibit hydrogen atoms that are dynamically disordered in two energetically nearly equivalent positions with similar occupational parameters (~0.5, entropically favored). The dielectric data of (β-CD)-Co at T < 220.0 K resemble those of the (β-CD)-M inclusion complexes with Ba^{2+}, Cd^{2+}, Li^+, K^+ and Cs^+ ions (6.0 ≤ $\Delta\varepsilon'$ ≤ 8.4, 0.7 ≤ ε''_{max} ≤ 1.4, T_{trans} = ~200.0 K) [11,12,50] implying that very few normal hydrogen bonds are transformed into flip-flop ones and a rather not extended flip-flop hydrogen-bonding network is produced. This behavior is opposed to the one of (β-CD)-Bi [17] whose dielectric study showed that the greatest per cent of normal hydrogen bonds was transformed into those of flip-flop type ($\Delta\varepsilon'$ = 49.6, ε''_{max} = 16.0, T_{trans} = 223.6 K) resulting in a high density flip-flop network which consisted of endless chains and many circular arrangements [49]. Furthermore, these results in combination with those obtained from FT-Raman spectroscopy and thermal analysis techniques suggested that apart from the Bi^{3+} ions the aforementioned network appeared to play a key role in limiting the Lewis base character of I^-_3. More specifically, the terminal and negatively charged I atoms of the I^-_3 ions seemed to close one or more flip-flop circular rings by accepting a certain number of disordered H-atoms which belonged to the vicinal O(6) hydroxyl groups. Such hydroxyl-iodide interactions have been also reported for other carbohydrate-polyiodide complexes [37,51].

Concerning (β-CD)-Co, the very low density flip-flop network indicates absence of structurally complicated hydrogen-bonding schemes almost eliminating the possibility of O(6)–H. . .I^-_3 interactions and revealing that the I^-_3 Lewis base character in the I^-_7 units which interact with the Co^{2+} ions is exclusively modified by the latter ones. This is further supported by the following facts: (i) in the I^-_7 units which display no interactions with the Co^{2+} ions the symmetric and full charge–transfer interaction $[I_2 \leftarrow I^-_3 \rightarrow I_2]$ during heating shows no involvement of the relevant I^-_3 ions in hydrogen-bonding, and (ii) even in the case of (β-CD)-Te [17] where a flip-flop network was formed with a much higher density ($\Delta\varepsilon' = 18.6$, $\varepsilon''_{max} = 4.8$, $T_{trans} = 216.8$ K) than the corresponding one of (β-CD)-Co, there was no experimental evidence for the existence of O(6)–H. . .I^-_3 interactions. At $T > 220.0$ K, both the $\varepsilon'(T)$ and $\varepsilon''(T)$ variations in Fig. 6a and b illustrate a well-distinguishable sigmoid curve which is followed by a rapid increase. The first experimental feature is ascribed to the transformation of a small per cent of tightly bound water molecules (fully occupied positions) to easily movable ones (distributed over specific positions) whereas the second one corresponds to the continuous transformation $(H_2O)_{tightly\ bound} \rightarrow (H_2O)_{easily\ movable}$ being consistent with proton transport and extensive dipole relaxation in the highly disordered interstitial water arrangement [19,20,52–54]. The latter processes are further accompanied by metal ion dislocations mainly emerging from the strong influence of the applied alternating field. All the intriguing phenomena described above have been thoroughly interpreted in our previous investigations [11–18].

4. Concluding remarks

In this work, via the employment of the temperature-dependent FT-Raman spectroscopy, we have been able to observe all the heptaiodide ($I_2 \cdot I^-_3 \cdot I_2$) structural conversions along with the relevant electron transfer phenomena in the polycrystalline β-cyclodextrin polyiodide inclusion complex $(\beta\text{-CD})_2 \cdot Co_{0.5} \cdot I_7 \cdot 21H_2O$ ((β-CD)-Co). The cobalt ions are found to exhibit a statistical distribution of 0.5 Co^{2+} per β-CD dimer indicating the coexistence of I^-_7 units which present no interactions with the Co^{2+} ions and I^-_7 units which interact with the Co^{2+} ions. The former units display a disorder–order transition of both their I_2 molecules at $T > 60\,^\circ$C due to a symmetric and full charge–transfer interaction with the central I^-_3 $[I_2 \leftarrow I^-_3 \rightarrow I_2]$, whereas in the case of the latter ones the situation is more complicated. More specifically, at $T > 30\,^\circ$C only one of the two disordered I_2 molecules gradually becomes elongated and well-ordered (disorder–order transition) due to a charge–transfer interaction with the central I^-_3. The other I_2 molecule remains in the disordered state exhibiting no charge–transfer interaction with I^-_3. Such behavior has not been observed in the previous studies of other β-CD metal-polyiodide complexes of the family ((β-CD)-M), where the I^-_3 ion was found to donate electron density to both the I_2 molecules of I^-_7. In the current research, the significant modification of the Lewis base character of I^-_3 ion is exclusively attributed to its specific interaction with the Co^{2+} ion. According to the obtained experimental results, the Co^{2+} ion appears to occupy a side-on position in relation to I^-_3 inducing a considerable asymmetry on the geometry and the electron donating properties of the latter ion. Therefore, it becomes explicit that by changing the nature of the metal ion we can achieve control of the underlying polyiodide charge–transfer processes. Additionally, it should be stressed that apart from the detection of all the above effects, FT-Raman spectroscopy proves to be of great importance for one more reason; it may even depict in detail the very slight differences in the structures of the disordered polyiodide subunits. Finally, complementary dielectric measurements support the existence of a limited flip-flop H-bonding network in (β-CD)-Co suggesting no important influence of H···I contacts on the electron transfer properties of I^-_3.

Acknowledgements

The authors are grateful to NKUA for partial financial support, Grant No. 70/4/3347SARG. Special thanks go to the staff of the Institute of Geology and Mineral Exploration (I.G.M.E.) for their skilled technical assistance concerning the compositional analyses of C, H and Co elements.

References

[1] J. Szejtli, Chem. Rev. 98 (1998) 1743–1753.
[2] E.R. Domb, D.J. Sellmyer, G.D. Sturgeon, J. Phys. Chem. Solids 40 (1979) 739–741.
[3] R.C. Teitelbaum, S.L. Ruby, T.J. Marks, J. Am. Chem. Soc. 102 (1980) 3322–3328.
[4] M. Mizuno, J. Tanaka, I. Harada, J. Phys. Chem. 85 (1981) 1789–1794.
[5] A. Oza, Phys. Stat. Sol. B 114 (1982) K171–K176.
[6] E.A. Rietman, Mater. Res. Bull. 25 (1990) 649–655.
[7] F. Cramer, U. Bergmann, P.C. Manor, M. Noltemeyer, W. Saenger, Justus Liebigs, Ann. Chem. 7/8 (1976) 1169–1179.
[8] M. Noltemeyer, W. Saenger, Nature 259 (1976) 629–632.
[9] M. Noltemeyer, W. Saenger, J. Am. Chem. Soc. 102 (1980) 2710–2722.
[10] Ch. Betzel, B. Hingerty, M. Noltemeyer, G. Weber, W. Saenger, J.A. Hamilton, J. Inclusion Phenom. 1 (1983) 181–191.
[11] V.G. Charalampopoulos, J.C. Papaioannou, Mol. Phys. 103 (2005) 2621–2631.
[12] V.G. Charalampopoulos, J.C. Papaioannou, H.S. Karayianni, Solid State Sci. 8 (2006) 97–103.
[13] J.C. Papaioannou, V.G. Charalampopoulos, P. Xynogalas, K. Viras, J. Phys. Chem. Solids 67 (2006) 1379–1386.
[14] V.G. Charalampopoulos, J.C. Papaioannou, K.E. Tampouris, Solid State Ionics 178 (2007) 793–799.
[15] V.G. Charalampopoulos, J.C. Papaioannou, Carbohydr. Res. 342 (2007) 2075–2085.
[16] V.G. Charalampopoulos, J.C. Papaioannou, G. Kakali, H.S. Karayianni, Carbohydr. Res. 343 (2008) 489–500.
[17] V.G. Charalampopoulos, J.C. Papaioannou, Solid State Ionics 179 (2008) 565–573.
[18] V.G. Charalampopoulos, J.C. Papaioannou, K. Viras, H.S. Karayianni, G. Kakali, Supramol. Chem. 22 (2010) 499–510.
[19] N. Nandi, K. Bhattacharyya, B. Bagchi, Chem. Rev. 100 (2000) 2013–2046.
[20] R. Pomes, B. Roux, Biophys. J. 82 (2002) 2304–2316.
[21] B.B. Owens, B. Pate, P.M. Skarstad, D.L. Worburton, Solid State Ionics 9/10 (1983) 1241–1245.
[22] P.H. Svensson, L. Kloo, Chem. Rev. 103 (2003) 1649–1684.
[23] J. Haller, U. Kaatze, J. Mol. Liq. 138 (2008) 34–39.
[24] L.B. Railsback, Geology 31 (2003) 737–740.
[25] W. Kraus, G. Nolze, J. Appl. Crystallogr. 29 (1996) 301–303.
[26] G. Nolze, W. Kraus, Powder Diffr. 13 (1998) 256–259.
[27] A. Anderson, T.S. Sun, Chem. Phys. Lett. 6 (1970) 611–616.
[28] P. Deplano, F.A. Devillanova, J.R. Ferraro, F. Isaia, V. Lippolis, M.L. Mercuri, Appl. Spectrosc. 46 (1992) 1625–1629.
[29] F. Demartin, P. Deplano, F.A. Devillanova, F. Isaia, V. Lippolis, G. Verani, Inorg. Chem. 32 (1993) 3694–3699.
[30] J.J. Novoa, F. Mota, S. Alvarez, J. Phys. Chem. 92 (1988) 6561–6566.
[31] G.A. Landrum, N. Goldberg, R. Hoffmann, J. Chem. Soc. Dalton Trans. (1997) 3605–3613.
[32] R.B. Girling, H.F. Shurvell, Vibrational Spectrosc. 18 (1998) 77–82.
[33] J.D. Dunitz, V. Schomaker, K.N. Trueblood, J. Phys. Chem. 92 (1988) 856–867.
[34] E.M. Nour, L.H. Chen, J. Laane, J. Phys. Chem. 90 (1986) 2841–2846.
[35] E.M. Nour, L.H. Chen, J. Laane, J. Raman Spectrosc. 17 (1986) 467–469.
[36] A. Sengupta, E.L. Quitevis, M.W. Holtz, J. Phys. Chem. B 101 (1997) 11092–11098.
[37] O. Nimz, K. Gebler, I. Usón, S. Laettig, H. Welfle, G.M. Sheldrick, W. Saenger, Carbohydr. Res. 338 (2003) 977–986.
[38] S.B. Sharp, G.I. Gellene, J. Phys. Chem. A 101 (1997) 2192–2197.
[39] P.H. Svensson, L. Kloo, J. Chem. Soc. Dalton Trans. (2000) 2449–2455.
[40] H. Mittag, H. Stegemann, H. Füllbier, G. Irmer, J. Raman Spectrosc. 20 (1989) 251–255.
[41] X. Yu, R.H. Atalla, Carbohydr. Res. 340 (2005) 981–988.
[42] S.M. Teleb, M.S. Refat, Spectrochim. Acta A: Mol. Biomol. Spectrosc. 60 (2004) 1579–1586.
[43] R. Yuan, Y.-Q. Chai, D. Lin, D. Gao, J.-Z. Li, R.-Q. Yu, Anal. Chem. 65 (1993) 2572–2575.
[44] R. Yuan, Y.-Q. Song, Y.-Q. Chai, S.-X. Xia, Q.-Y. Zhong, B. Yi, M. Ying, G.-L. Shen, R.-Q. Yu, Talanta 48 (1999) 649–657.
[45] J. Dai, Y. Chai, R. Yuan, X. Zhong, Y. Liu, D. Tang, Anal. Sci. 20 (2004) 1661–1665.
[46] E.L. Muetterties, Inorg. Chem. 4 (1965) 769–771.
[47] J.R. Macdonald, Impedance Spectroscopy, Wiley, New York, 1987, pp. 1–26.

[48] W. Saenger, Ch. Betzel, B. Hingerty, G.M. Brown, Nature 296 (1982) 581–583.
[49] Ch. Betzel, W. Saenger, B.E. Hingerty, G.M. Brown, J. Am. Chem. Soc. 106 (1984) 7545–7557.
[50] J.C. Papaioannou, Mol. Phys. 102 (2004) 95–99.
[51] Z. Peralta-Inga, G.P. Johnson, M.K. Dowd, J.A. Rendleman, E.D. Stevens, A.D. French, Carbohydr. Res. 337 (2002) 851–861.
[52] N. Agmon, Chem. Phys. Lett. 244 (1995) 456–462.
[53] E.P. Quigley, P. Quigley, D.S. Crumrine, S. Cukierman, Biophys. J. 77 (1999) 2479–2491.
[54] B.V. Merinov, Solid State Ionics 84 (1996) 89–96.